



Lawrence Berkeley Laboratory

UNIVERSITY OF CALIFORNIA

Materials & Molecular Research Division

Submitted to *Physica Status Solidi*

THE ORIGIN OF Mo_2C PRECIPITATE MORPHOLOGY IN MOLYBDENUM

J.M. Lang, U. Dahmen, and K.H. Westmacott

September 1982

TWO-WEEK LOAN COPY

*This is a Library Circulating Copy
which may be borrowed for two weeks.
For a personal retention copy, call
Tech. Info. Division, Ext. 6782.*



LBL-14970
c. 2

DISCLAIMER

This document was prepared as an account of work sponsored by the United States Government. While this document is believed to contain correct information, neither the United States Government nor any agency thereof, nor the Regents of the University of California, nor any of their employees, makes any warranty, express or implied, or assumes any legal responsibility for the accuracy, completeness, or usefulness of any information, apparatus, product, or process disclosed, or represents that its use would not infringe privately owned rights. Reference herein to any specific commercial product, process, or service by its trade name, trademark, manufacturer, or otherwise, does not necessarily constitute or imply its endorsement, recommendation, or favoring by the United States Government or any agency thereof, or the Regents of the University of California. The views and opinions of authors expressed herein do not necessarily state or reflect those of the United States Government or any agency thereof or the Regents of the University of California.

The Origin of Mo_2C Precipitate Morphology in Molybdenum†

J.M. Lang*, U. Dahmen and K.H. Westmacott

Materials and Molecular Research Division

University of California

Lawrence Berkeley Laboratory

Berkeley, CA 94720

September 1982

*This work was supported by the Director, Office of Energy Research,
Office of Basic Energy Sciences, Materials Sciences Division of the U.S.
Department of Energy under Contract No. DE-AC03-76SF00098.

†Presently at Aluminium Pechiney, B.P. 24, 38340 Voreppe, France

A detailed electron metallographic analysis has been conducted on the morphology and interface structure of Mo_2C precipitates in a quenched and aged Mo-C alloy. The precipitates were found to be plate-shaped and to lie on $\{301\}$ matrix planes. The approximate Burgers orientation relationship, $(0001) \parallel (110)$, $[\bar{1}2\bar{1}0] \parallel [\bar{1}11]$, was confirmed. Characteristic striations along $\langle\bar{1}13\rangle$ matrix directions in the interface were analyzed as slip traces of shear loops on the basal plane.

The overall features of the precipitate morphology are explained in terms of a model based on the invariant line concept. The invariant plane strain condition of a planar interface is met by the periodic nucleation of shear loops to relieve the developing stresses. An observed small misorientation between the close-packed planes is a consequence of the restraints imposed on the precipitate by the surrounding matrix. Good agreement is also found between the model and independent observations on other refractory metal interstitial alloy systems.

1. INTRODUCTION

The growth of plate-shaped precipitates is found in many instances to proceed by a ledge mechanism [1]. The kinetic and structural aspects of ledge growth have been studied in model systems such as Al-Cu [2,3] and an improved understanding of the growth mechanisms is developing [4].

In contrast, there are few systematic studies of precipitate plate growth by non-ledge mechanisms. Systems identified to be in this category include most transition metal carbon and nitrogen alloys which are of great technological interest.

In these alloys a carbide or nitride phase of fcc or hcp structure precipitates in a bcc matrix. As a result there is usually no pair of low-index planes with nearly perfect match as is found in other systems, e.g. $\{111\}_{\text{fcc}} \parallel (0001)_{\gamma}$, in Al-Ag or $\{001\}_{\text{fcc}} \parallel \{001\}_{\text{g}}$ in Al-Cu. In the absence of such "natural coherency", expressed as an invariant plane transformation strain (IPS), precipitate thickening cannot proceed by ledges.

In many of these systems the transformation strain can be made into an invariant line strain (ILS) if during the transformation an appropriate orientation relationship (OR) is established [5]. This has been observed experimentally for a great number of alloy systems. Both lateral growth and thickening of a plate-shaped precipitate under these conditions will be distinctly different from the ledge growth of an IPS-produced plate. The present study focusses on one such system, Mo-C, and the precipitation of hcp Mo_2C plates in the bcc lattice.

Mo-C alloys have received recent attention in an effort to understand the influence of interstitial elements on the embrittlement of transition metals. Kumar and Eyre [6] used transmission electron microscopy to study the crystallography of both intra- and intergranular precipitates of Mo_2C in slowly cooled Mo. They found an OR close to the Burgers relationship [7], and using Moire fringes they detected a small misorientation between $(0001)_{\text{Mo}_2\text{C}}$ and $(110)_{\text{Mo}}$. They concluded that interface boundaries were located on planes in $\langle 110 \rangle_{\text{Mo}}$ zones and analyzed interfacial dislocation networks with unusual $a/2\langle 110 \rangle$ Burgers vectors. The problem of embrittlement also prompted Florjančić to study in detail the heterogeneous precipitation of Mo_2C in Mo grain boundaries [8]. He found precipitates on $\{111\}$, $\{112\}$ and $\{123\}_{\text{Mo}}$ habit planes, often leading to a

sawtooth structure of the grain boundary. An extensive study of the entire sequence of precipitation in rapidly quenched Mo-C single crystals was made by Burck [9] who found small coherent precipitates on $\{114\}_{\text{Mo}}$ planes which developed into semicoherent plates during high temperature aging. He confirmed the Burgers OR of Kumar and Eyre's work but did not report the small misorientation between close-packed planes. In large precipitates he observed a planar substructure which he interpreted as twinning on $\{\bar{1}011\}_{\text{Mo}_2\text{C}}$ planes.

A comparison between Mo-C and other transition metal interstitial alloys shows close similarities [5]. The hexagonal precipitates in V-C [10], V-N [11], Nb-C [12], Nb-N [13], Ta-C [14], Ta-N [13], W-C [15] and Fe-Cr-N [16] all follow the Burgers or the very closely related Potter OR [11]. With few exceptions, precipitate plates form on $\{301\}$ matrix planes. In fact, $\{301\}$ habit planes were found even for fcc carbides and nitrides such as TiC and TiN in Mo [17]. Thus it appears that the habit plane of all these precipitates is determined by crystallographic considerations and this suggests a similar behavior for Mo_2C precipitates in Mo.

The Mo-C alloy was therefore chosen as a model system for studying plate-shaped precipitates related to the surrounding matrix by an ILS. A systematic TEM investigation of the crystallography of Mo_2C precipitation is presented and the results are explained by a general model for the growth and accommodation of ILS-produced precipitates.

2. EXPERIMENTAL PROCEDURES

The materials were prepared from Molybdenum ribbons supplied by Johnson, Matthey and Co.. The main substitutional impurities are iron (< 20 at. ppm) and chromium (< 10 at. ppm). Interstitial impurities are carbon, nitrogen and oxygen which are at a level less than 100 at. ppm in the untreated samples. The strips were cold rolled to a thickness of 150 μ m, and homogenized by Joule heating in an ultra-high vacuum furnace (10^{-6} Pa) at 2600K. During such a heat treatment oxygen, nitrogen and hydrogen outgas to levels below 10 at. ppm [9]. At the same time the rolled strip recrystallizes into large grains with a preferred orientation so that the <100> axis is perpendicular to the plane of the foil. The specimens were then heated to 1900K in a known volume of acetylene ($\sim 1\ell$) at a given pressure (10^{-2} Pa). This treatment resulted in the carbon absorption in the sample to an estimated concentration of 500 to 5000 at. ppm. While adequate for the study of structural features of precipitation, this procedure is not suitable for quantitative studies.

To prevent heterogeneous nucleation on grain boundaries, the sample was quenched at a cooling rate of $\sim 2500 \text{ Ks}^{-1}$ (measured with a 75 μ m tungsten-rhenium thermocouple and an oscilloscope) by switching off the heating current. The specimens were then annealed in the same UHV system for 1 h at 1073K.

2.1. Electropolishing. From the carburized and annealed strip 2.3mm discs were punched out and electropolished in a methanol, glycerol, sulfuric acid (80%, 16%, 4% by volume) solution at -35°C and 30V. Adding glycerol resulted in a slower but

better polish than without glycerol, and reduced the preferential etching out of large Mo_2C precipitates.

2.2 Electron Microscopy. A Philips 301 was used for conventional microscopy, a JEOL 200CX for high resolution, a Philips 400 for convergent beam experiments, and a 1.5MeV Kratos HVEM to obtain good penetration in thick foils.

3. EXPERIMENTAL RESULTS

3.1. Orientation Relationship. To determine the orientation relationship the convergent beam technique was used on relatively big precipitates protruding from the edge of the foil. The electron beam size (50 nm) and the convergence angle ($5 \cdot 10^{-3}$ rd) was such that Kikuchi lines were obtained from the precipitate only. This allowed the beam to be oriented along a low order zone axis with very good precision (Fig. 1a). By next translating the probe on to the nearby matrix without moving the specimen (Fig. 1b), the relative orientation could be determined with an accuracy of at least 0.5° .

As shown in Fig. 1, using a short diffraction constant very clearly reveals the angular distance between the $[001]_{\text{Mo}}$ and $[\bar{2}110]_{\text{Mo}_2\text{C}}$ axes corresponding to a rotation of $5.2 \pm 0.5^\circ$ around the $[110]_{\text{Mo}}$ axis. The orientation is approximately the Burgers OR as shown in the stereogram of Fig. 2. A small misalignment of $[110]_{\text{Mo}}$ and $[0001]_{\text{Mo}_2\text{C}}$ (not shown in Fig. 2) reported in ref. [6] was precisely measured in a high resolution lattice image of a precipitate interface and found to be 2° . A similar result was reported for the Ta-C system [14]. This small rotation brings $(\bar{1}011)_{\text{Mo}_2\text{C}}$ into coincidence with $(101)_{\text{Mo}}^*$ and changes the Burgers to the Potter orientation relationship [11]. These results

* Whenever specific indices are used, they refer to Fig. 2.

were also found to be true for smaller platelike precipitates as shown by microdiffraction in Fig. 5f.

3.2. Morphology of the semicoherent carbides. Fig. 3a shows the morphology of hcp Mo_2C platelets in the bcc Mo matrix. Typical dimensions were 500nm in diameter and 20nm in thickness. The habit plane was determined by tilting the precipitates edge-on. As the density of platelets was rather low, the improved penetration offered by high voltage microscopy was helpful in selecting a precipitate suitable for analysis. Moreover, it was easier to decide when a precipitate was edge-on. Precision was increased by imaging under weak beam conditions to minimize the strain contrast surrounding the plates.

In Fig. 3 it can be seen that one platelet (A) is edge-on for both the $[\bar{1}03]$ and $[\bar{1}13]$ beam directions; the habit plane was thus uniquely determined to be $(301)_{\text{Mo}}$. The habit plane normal and its trace are shown stereographically in Fig. 2.

3.3. Analysis of Interfacial Lines. The broad faces of the precipitates were covered with an array of remarkably straight lines (Figs. 3, 4). Knowing that they were located in the interface, they were determined to lie along $[\bar{1}13]_{\text{Mo}}$ by trace analysis (for example, for the (301) plate, they are parallel to $[200]$ with beam direction $B = [013]$). Fig. 2 illustrates this direction relative to the (301) habit plane and the (0001) basal plane of the precipitate.

Fig. 4 shows a high magnification picture of one such nearly face-on platelet. The lines are paired corresponding to the top and bottom surfaces of the precipitate bounding regions of light and dark contrast. One can see an indentation

(A) at the edge and a "nose" (B) out of the plane of the precipitate. Both of these features were observed quite often.

The strain in the matrix neighboring the platelet was determined by a $g \cdot b$ analysis as shown in Figs. 5a,b,c. The lines are visible when using the 002 reflection (a) but are out of contrast when using an $0\bar{3}\bar{1}$ (b) and an 020 reflection (c). Thus, the strain in the matrix has a displacement vector with a strong component along [001]. The remaining strain is probably along [100] since it was found to be invisible with beam directions close to [100].

The contrast behavior of the precipitate itself is often obscured by matrix effects (i.e. Moiré fringes and strain contrast) but valuable information can be gained by microdiffraction.

Fig. 5f is the microdiffraction pattern of Fig. 5e. It can be seen that $B = [\bar{1}\bar{1}3]_{\text{Mo}} \approx [\bar{1}\bar{1}00]_{\text{Mo}_2\text{C}}$ and that there is a rotation along this zone axis so that [0001] is not exactly parallel to [110] as has been noted previously for bigger precipitates. For simplicity, this misorientation is not shown in the stereogram (Fig. 2). In Fig. 5e the precipitate is seen edge-on along $[\bar{1}\bar{1}3]$ which is the direction of the interfacial lines. It is also evident from this image that the cross-section of the platelet is striated with lines which run perpendicular to the [0001] direction.

From this $[\bar{1}\bar{1}00]$ zone, the precipitate was tilted to $[\bar{2}\bar{1}10]$ using the matrix reflections as a navigational aid. The $[\bar{2}\bar{1}10]$ pattern, instead of well-defined

spots, consists of streaks perpendicular to the (0001) plane, with no spots or streaks in the (0001) systematic row.

This situation can be analysed in the simplified manner recently proposed [18]. Instead of describing matrix and precipitate spots separately, they can be described as product and parent lattices related by a shear; in the reciprocal lattice the invariant plane has a normal \vec{s} , and a shear direction \vec{n} which corresponds in the direct lattice to a shear of direction \vec{s} leaving a plane with normal \vec{n} invariant.

Fig. 5d is interpreted in real space as a shear along $[\bar{1}2\bar{1}0]$ in the (0001) plane. Streaks instead of spots are observed because the shear \vec{s} is accomplished by a set of dislocations that are not perfectly periodically spaced.

3.4. Dislocations in the matrix associated with the precipitate. Many of the precipitates were hidden in a tangle of dislocations making a detailed analysis difficult. However, some of the observed features appeared to be general. Dislocation loops such as the ones visible in Fig. 3 were found to lie in planes (probably $\{110\}$) near the $\{301\}$ habit plane of the precipitate. These dislocations had $\frac{a}{2}\langle 111 \rangle$ type Burgers vectors and were pinned at the edges of the platelets.

4. DISCUSSION

The most illuminating way to discuss the present results is in terms of the concept of an invariant line [5]. As shown in Fig. 6, an hcp cell can be produced out of a bcc cell by strains along the three principal axes x, y, z and a shuffle of

the atoms in every other layer normal to the z-axis (shaded atoms). This transformation is analyzed here for the Mo-Mo₂C case with $a_{\text{bcc}} = 0.3147$ nm, $a_{\text{hcp}} = 0.3002$ nm, $c_{\text{hcp}} = 0.4724$ nm, $c/a = 1.57$ [19]. The transformation matrix A refers to the axes

$$\begin{aligned} (x, y, z) &= ([00\bar{1}]_{\text{bcc}}, [\bar{1}10]_{\text{bcc}}, [110]_{\text{bcc}}) \\ &= ([2\bar{1}\bar{1}0]_{\text{hcp}}, [01\bar{1}0]_{\text{hcp}}, [0001]_{\text{hcp}}) . \end{aligned}$$

In this coordinate system the transformation matrix is

$$A = \begin{pmatrix} 0.95 & 0 & 0 \\ 0 & 1.17 & 0 \\ 0 & 0 & 1.06 \end{pmatrix} = \begin{pmatrix} a & 0 & 0 \\ 0 & b & 0 \\ 0 & 0 & c \end{pmatrix}$$

a, b, c being constants defined by this relation.

An invariant line \underline{u} can be obtained by a rotation through an angle θ , (to be determined), around the $z = [110]$ bcc axis. This can be expressed by

$$A' = \begin{pmatrix} \cos \theta & \sin \theta & 0 \\ -\sin \theta & \cos \theta & 0 \\ 0 & 0 & 1 \end{pmatrix} \begin{pmatrix} a & 0 & 0 \\ 0 & b & 0 \\ 0 & 0 & c \end{pmatrix} = \begin{pmatrix} a \cos \theta & b \sin \theta & 0 \\ -a \sin \theta & b \cos \theta & 0 \\ 0 & 0 & c \end{pmatrix}$$

and $A'u = u$, that is $\det |A' - I| = 0$ for a nontrivial solution [5]. When solved, this equation gives $\cos \theta = \frac{1 + ab}{a+b} = 9.963 \times 10^{-1}$ and $\theta = 4.9^\circ$

$$A' = \begin{pmatrix} 0.950 & -0.098 & 0 \\ 0.081 & 1.164 & 0 \\ 0 & 0 & 1.06 \end{pmatrix}$$

The solution of the equation $A'u = u$ is the vector

$$\begin{pmatrix} -0.90 \\ 0.43 \\ 0 \end{pmatrix}$$

in the (x, y, z) coordinate system. In terms of the crystallographic axes, this vector is $[\bar{1}13]_{M_0}$ which is indeed the observed direction of interfacial lines.

An invariant line is thus produced by a rotation of 4.9° around $[110]_{M_0}$ (instead of 5.26° corresponding to the exact Burgers OR shown in Fig. 2). Within the limits of the experimental precision this is the observed OR as illustrated in Fig. 1. Thus it can be concluded, as suggested earlier [14], that the OR between the matrix and the precipitate lattice is such that there is a line of no strain, i.e. an invariant line.

4.1. Model. If the precipitate/matrix interface contains this invariant line direction (here $[\bar{1}13]$) one condition for a low energy interface is met. It was shown in [20] that needles of bcc Cr in fcc Cu followed the same invariant line criterion. However, in the present case, the precipitates are plates rather than

needles. The observation of the unusual closely spaced interfacial lines along the invariant line direction suggests they are related to this change from needle to plate shape. A credible model evolves naturally from a consideration of likely mechanisms for this transition. The transformation stresses which build up whenever the precipitate grows normal to its zero strain axis can be relieved by the periodic nucleation and expansion of a shear loop [20]. The loop plane must contain both the Burgers vector and the invariant line and will generally be inclined to the habit plane. As a result the precipitate plate will be enveloped by a parallel set of shear loops lying in the interface. Because of the plate shape of the precipitates the appearance of the shear loops in most orientations will be one of dipoles along the invariant line. This explains the observed pairing of the interfacial lines across the precipitates (see Fig. 4).

The plane of the shear loops can be seen directly when the precipitate is viewed along the invariant line direction as shown in Fig. 5e and the analysis revealed this shear plane to be the expected (0001) basal plane of the precipitate. In reciprocal space, the diffraction pattern shown in Fig. 5d exhibits splitting of the precipitate spots in the [0001] direction, normal to the plane of shear, whereas all the spots in the plane perpendicular to the $[\bar{1}2\bar{1}0]$ direction are unaffected. This method of analysis [18] allows a simple direct identification of the shear system as (0001)/ $[\bar{1}2\bar{1}0]$. The stereogram in Fig. 2 shows that in the Burgers OR this is a shear system common to matrix and precipitate. In the terminology of Olson and Cohen [21] the shear loops are (perfect) anticompatibility dislocations, and the resulting shear is lattice invariant. The reason this shear nevertheless leads to a splitting of the precipitate spots in the diffraction pattern is the ordering of carbon atoms in Mo_2C [19]. The array of shear loops will result in a

periodic sequence of (0001) antiphase boundaries as seen in Fig. 4. The continuous nature of the spot splitting is evidence for an imperfect periodicity of the antiphase boundaries.

It can thus be concluded that the growing precipitate relieves the coherency stresses by nucleating shear loops on the (0001) precipitate slip plane with a Burgers vector in the $[\bar{1}2\bar{1}0] \parallel [\bar{1}11]$ direction. The resulting stress relief is incomplete, however, since not all the homogeneous (lattice variant) strain lies in this direction. Hence the shear loops will be visible in an electron micrograph due to the net residual strains, i.e. the difference between the lattice variant and the lattice invariant strains. This explains the initially puzzling observation of an [001] component in the Burgers vector of the interfacial lines.

4.2. The deviation from the Burgers OR. The small but consistently observed deviation from the Burgers OR by misorientation between the close packed planes $(110)_m$ and $(0001)_p$ may also be understood in this model of precipitate growth. As the precipitate loses coherency by continued nucleation of shear loops, the highest stress relief occurs for the (301) habit plane. At the same time the constraint of the surrounding matrix lattice results in a rotation of the precipitate lattice much the same as in a single crystal tensile test with a single slip system operating. The magnitudes of shear and rotation are directly related and a complete quantitative analysis is in progress.

For the c/a ratio of the Mo_2C , only a small rotation is necessary to bring into coincidence $(\bar{1}011)$ and (101) to form the Potter OR [5]. Two precipitate variants related by a (101) mirror operation of the cubic matrix lattice would then be in

exact twin orientation with the twinning system $K_1 = (\bar{1}011)$, $\eta_1 = (1\bar{1}02)$. Partial strain accommodation can thus be achieved with twin related precipitates.

Finally, the dislocations surrounding the precipitates (Fig. 3) are thought to accommodate strains that build up as the precipitate grows in thickness (as opposed to lateral growth). Their behavior is different from that of the shear loops since only part of these loops lies in the interface and the remainder is free to expand in the matrix in response to elastic stresses.

4.3. Relation to other precipitation systems. Although the model for the precipitate growth and strain accommodation is discussed only for the Mo-C system, its application is much more general. $\{301\}$ habit planes have been reported not only for plate precipitates in a number of similar alloys such as V-C [10], Nb-C [12], Ta-C [14], but also for systems where the precipitating phase is fcc such as TiC and TiN in Mo [17]. As outlined in [5] the common factors are the transformation strains, the shear systems, and the requirement of an invariant line. If for the same crystallography, the lattice parameters are such that an invariant line cannot be formed, $\{001\}$ habits and more symmetric ORs are observed. This is the case for both hcp/bcc systems such as Mo_2C in Fe [22] and fcc/bcc systems such as HfC, HfN, ZrC, ZrN in Mo [17]. This clear pattern confirms an earlier suggestion that the $\{301\}$ habit planes are a result of crystallography rather than elastic anisotropy [14]. Other observations on large carbide particles confirm the precipitates slip plane of the present model. In Nb-C, V-C and to a lesser degree in Ta-C, extensive faulting was found on the precipitate (0001) planes.

A significantly different habit plane, $\{211\}$ instead of $\{301\}$ was observed in V-N [11] where the transformation strains are accommodated by twinning on $\{\bar{1}011\}$

rather than slip on (0001). Of all the hcp/bcc and fcc/bcc alloy systems listed above, this is the only one to exhibit extensive twinning and also the only one with a {211} habit. This is clear evidence for the important role of the mode of strain accommodation, slip or twinning, in the determination of the habit plane. Thus the model is supported by observations on a variety of alloy systems. The precipitate habit plane and resulting interface also conforms to the "minimum energy" criterion of O-lattice theory [23], the invariant plane strain/mobile interface requirement of martensite theory [24] as well as Eshelby's minimum strain energy criterion [25]. It has been shown [26,20] that this is not coincidental and the present study gives direct evidence for such interfaces.

5. CONCLUSIONS

- 1) Plate shaped precipitates of Mo_2C were found to form on {301} habit planes of the Mo matrix.
- 2) The observed orientation relationship was such that the matrix and precipitate lattices were related by an invariant line strain with $\langle \bar{1}13 \rangle$ as the invariant line direction.
- 3) Closely spaced lines in the precipitate interface plane lying along the direction of the invariant line were analyzed as shear dislocation loops.
- 4) Based on the strain accommodation by nucleation of these shear loops on (0001) planes with Burgers vector along $\langle \bar{1}2\bar{1}0 \rangle$ directions, a model is presented for the mechanism of precipitate growth.
- 5) The model explains the small misorientation between $(0001)_{\text{Mo}_2\text{C}}$ and $(110)_{\text{Mo}}$ by constrained shear on a single slip system.

- (6) Strain accommodation by periodic twinning on $\{\bar{1}011\}$ planes rather than by shear loops on the (0001) plane leads to a $\{211\}$ rather than a $\{301\}$ habit plane.

ACKNOWLEDGEMENTS

One of us (JML) gratefully acknowledges receipt of an I.R.S.I.D. scholarship. This work was supported by the Director, Office of Energy Research, Office of Basic Energy Sciences, Materials Sciences Division of the U. S. Department of Energy under Contract No. DE-AC03-76SF00098.

REFERENCES

1. H. I. AARONSON, "The Decomposition of Austenite by Diffusional Processes", ASM, Metals Park, Ohio (1970), p. 313.
2. P. MERLE and J. MERLIN, Acta Met. 29, 1929 (1981).
3. U. DAHMEN and K. H. WESTMACOTT, submitted to Acta Met.
4. H. I. AARONSON, Trans. Ind. Inst. Metals 32, 1 (1979).
5. U. DAHMEN, Acta Met. 30, 63 (1982).
6. A. KUMAR and B. L. EYRE, Acta Met. 26, 569 (1978).
7. W. G. BURGERS, Physica 1, 561 (1934).
8. M. FLORJANČIČ, M. S. Thesis, University of Stuttgart (1979).
9. P. BURCK, Ph. D. Thesis, Freiberg (1977).
10. D. R. DIERCKS and C. A. WERT, Met. Trans. 3, 1699 (1972).
11. D. I. POTTER, J. Less-Comm. Met. 31, 299 (1973).
12. R. K. VISWANADHAM and C. A. WERT, J. Less-Comm. Met. 48, 135 (1976).

13. A. DESCHANVRES, A. MAISSEU, G. NOUET and J. VICENS, *J. Less-Comm. Met.* 34, 237 (1974).
14. U. DAHMEN, K. H. WESTMACOTT and G. THOMAS, *Acta Met.* 29, 627 (1981).
15. R. A. SWALIN, *Acta Cryst.* 10, 473 (1957).
16. K. A. BYWATER and D. J. DYSON, *Metal Sci. J.* 9, 155 (1975).
17. N. E. RYAN, W. A. SOFFA and R. CRAWFORD, *Metallography* 1, 195 (1968).
18. U. DAHMEN and K. H. WESTMACOTT, *Proc. Int. Conf. on Electron Micr., Hamburg* (1982), vol. 2, p. 119.
19. L. E. TOTH, "Transition Metal Carbides and Nitrides", Academic Press, N. Y. (1971).
20. U. DAHMEN and K. H. WESTMACOTT, *Proc. Conf. Solid-Solid Phase Transf., Pittsburgh* (1981), in press.
21. G. B. OLSON and M. COHEN, *Acta Met.* 27, 1907 (1979).
22. D. J. DYSON, S. R. KEOWN, D. RAYNOR and J. A. WHITEMAN, *Acta Met.* 14, 867 (1966).
23. W. BOLLMANN, "Crystal Defects and Crystalline Interfaces", Springer, N. Y. (1970).
24. C. M. WAYMAN, "Introduction to the Crystallography of Martensitic Transformations", MacMillan, N. Y. (1964).
25. J. W. ESHELBY, *Proc. Roy. Soc. (A)* 341, 376 (1957).
26. J. W. CHRISTIAN, *Supplement to Trans. J. I. M.* 17, 21 (1976).

Fig. 1. Determination by convergent beam diffraction of the precise orientation relationship of an hcp Mo_2C precipitate in a bcc Mo matrix.

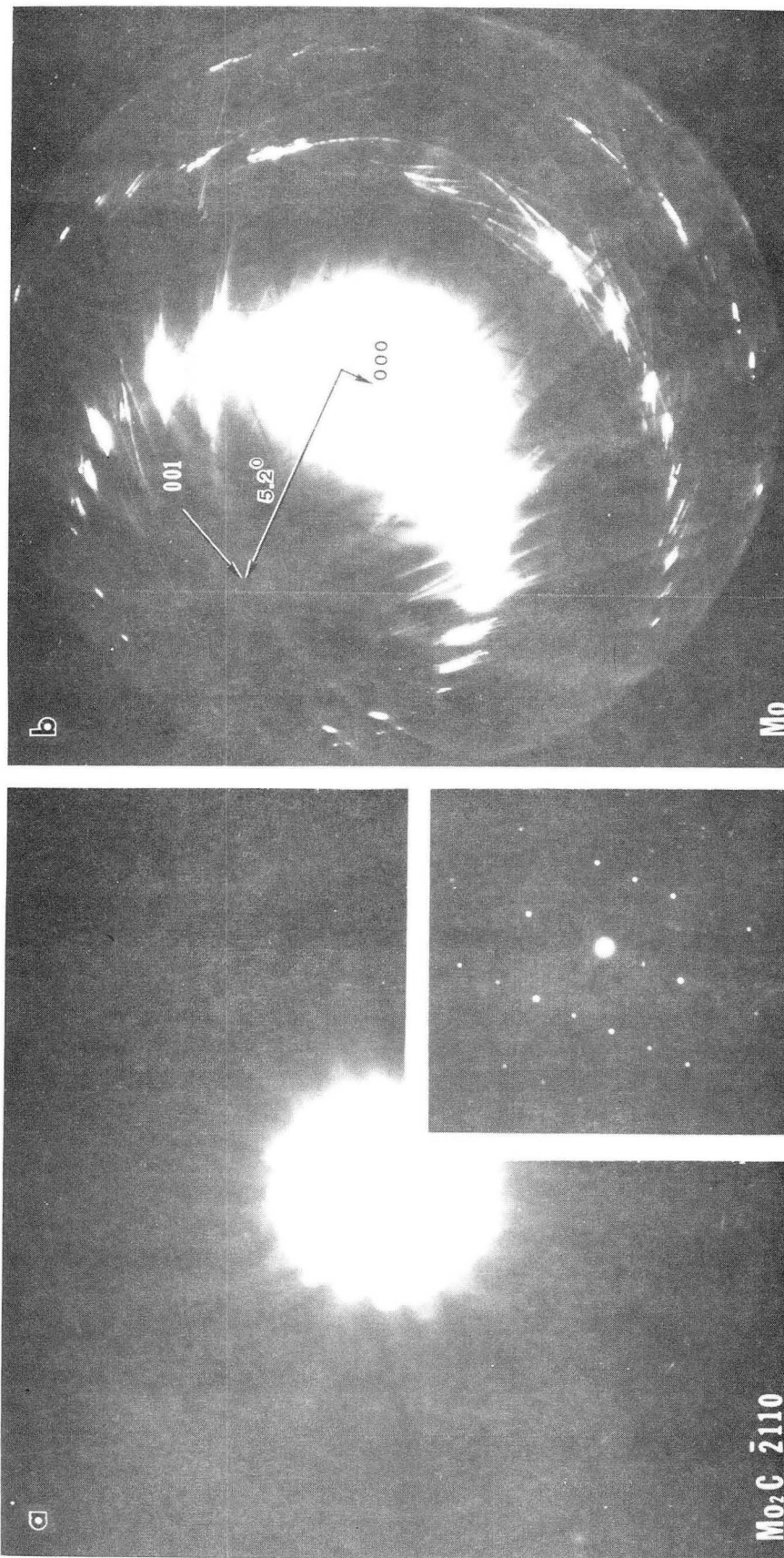
Fig. 2. Composite stereogram showing the Burgers OR which is approximately the OR between Mo_2C (hcp) ($c/a = 1.57$) and Mo (bcc). All specific indices used in the text refer to this figure.

Fig. 3. Tilting experiment determining the habit plane and the direction of interfacial lines on Mo_2C platelets. (700kV)

Fig. 4. High magnification image of a typical Mo_2C platelet. Arrows show respectively an indentation (A) and a "nose" (B) in the precipitate.

Fig. 5. a), b), c): Analysis of the strain field in the matrix surrounding a platelet. This strain field has a strong component along $[001]$. d) Microdiffraction pattern along $[\bar{2}110]_{\text{Mo}_2\text{C}}$ showing evidence of shear in the (0001) plane along the $[\bar{1}2\bar{1}0]_{\text{Mo}_2\text{C}}$ direction. e) Bright field image showing that the shear plane is $(0001)_{\text{Mo}_2\text{C}}$. f) Microdiffraction pattern of e); the precipitate spots are outlined. The arrow points to the small rotation of $(0001)_{\text{Mo}_2\text{C}}$ away from $(110)_{\text{Mo}}$.

Fig. 6. Schematic showing lattice correspondence between bcc cell (heavy outlines) and hcp cell. Every other layer of atoms normal to the z-axis (shaded) must undergo a small shuffle.



XBB 828-6926

Fig. 1

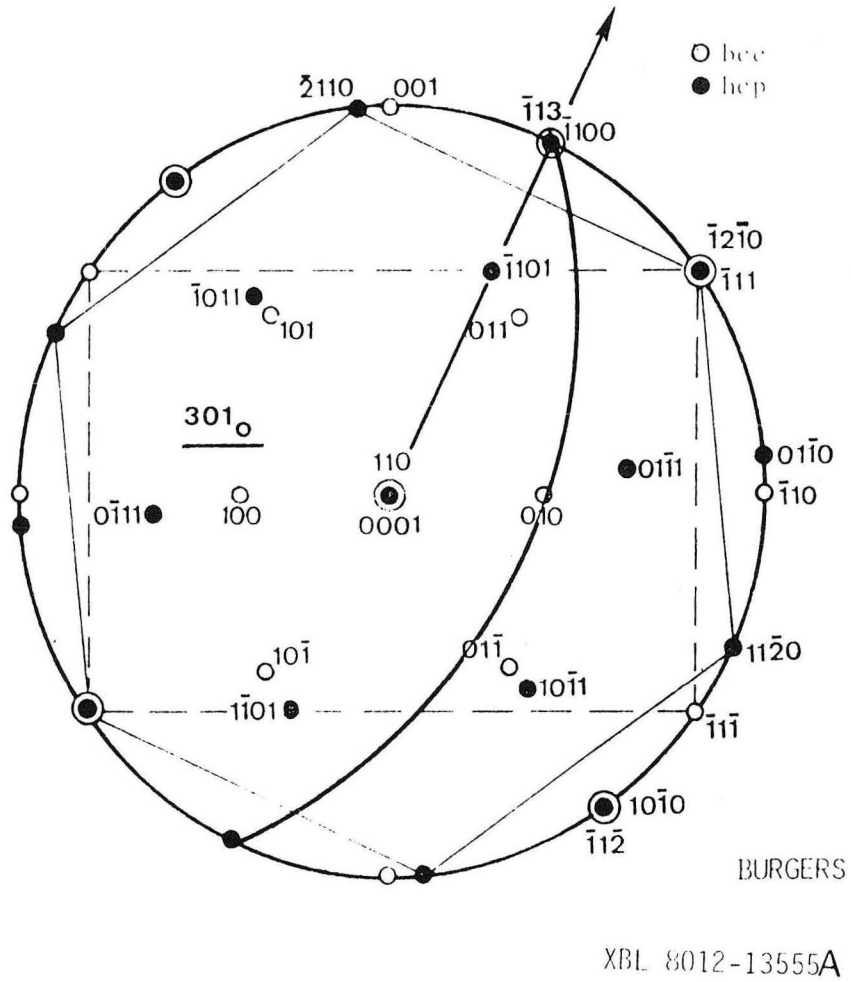
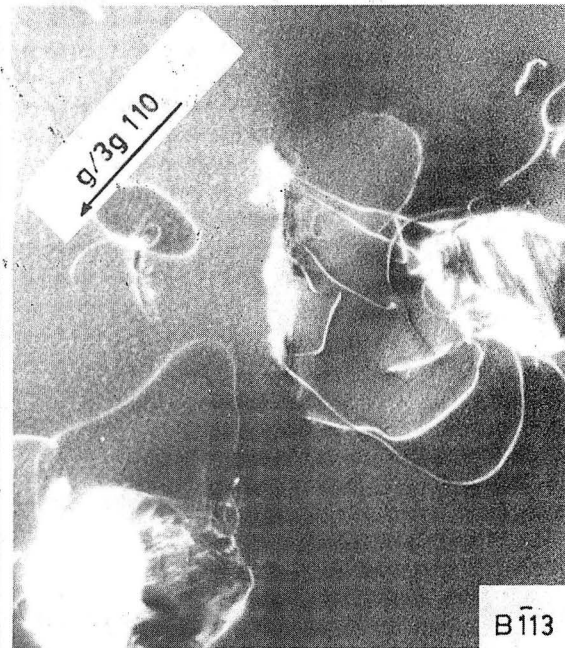
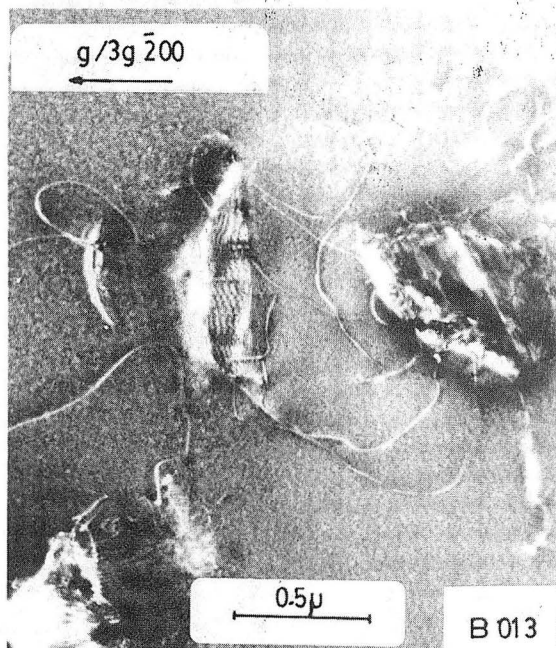
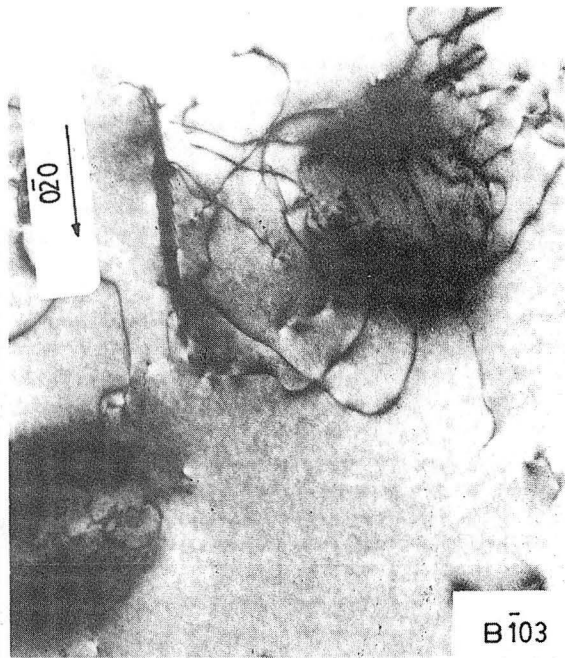
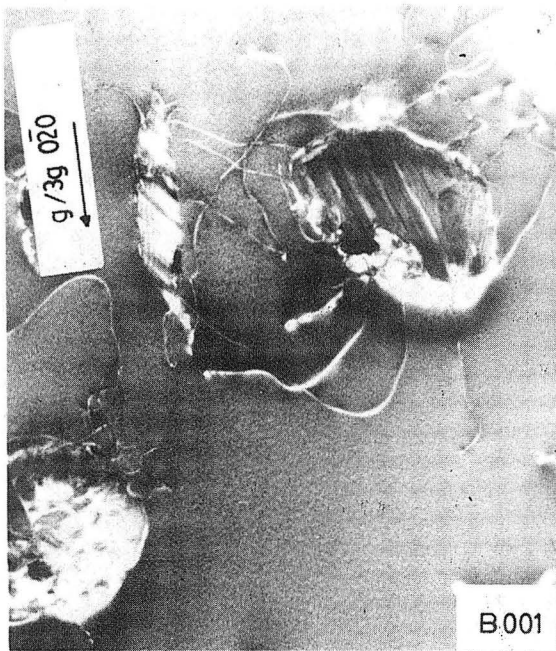
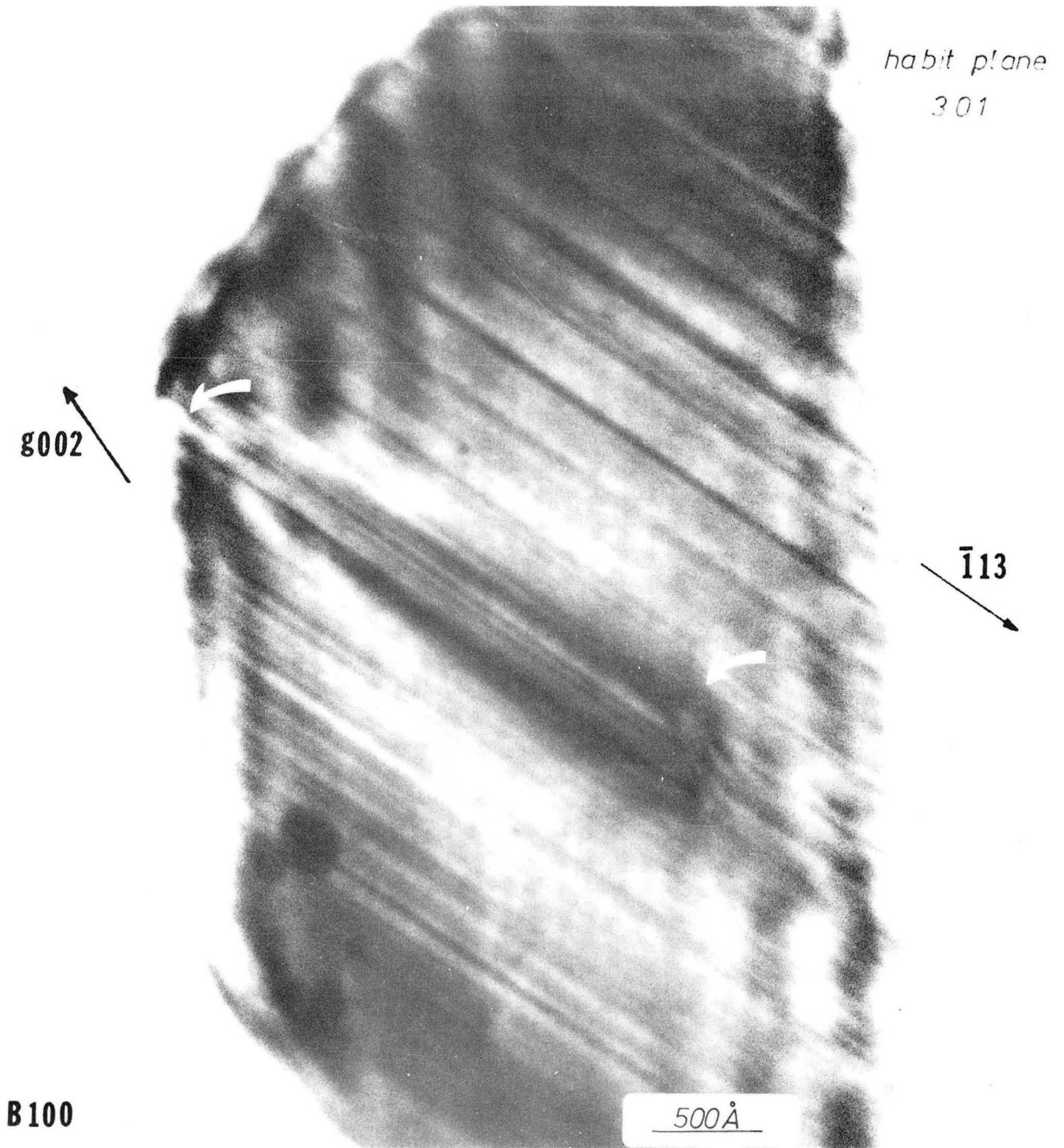


Fig. 2



XBB 823-2111

Fig. 3



XBB 823-2109

Fig. 4

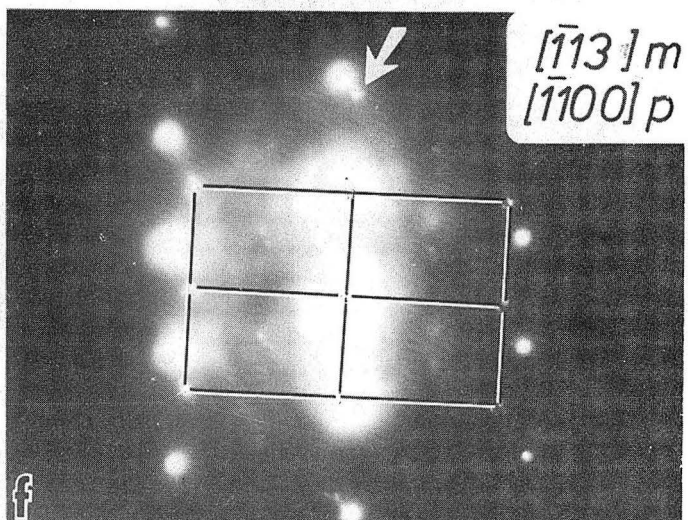
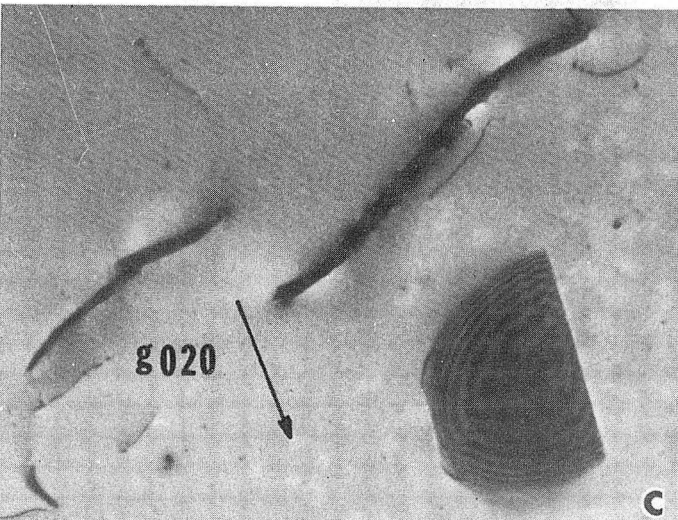
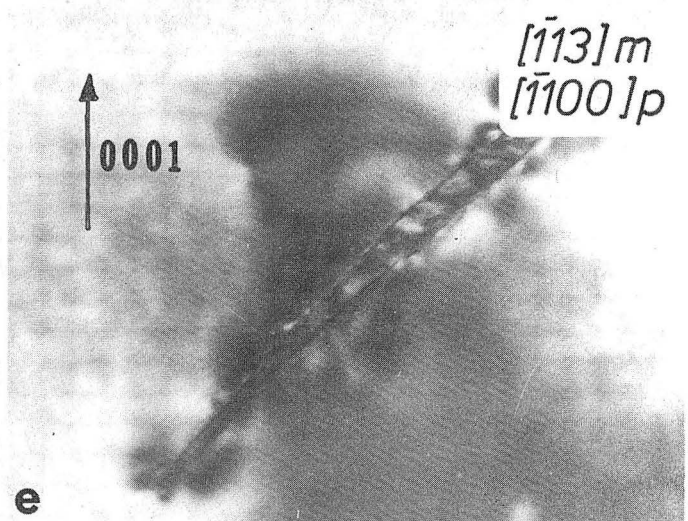
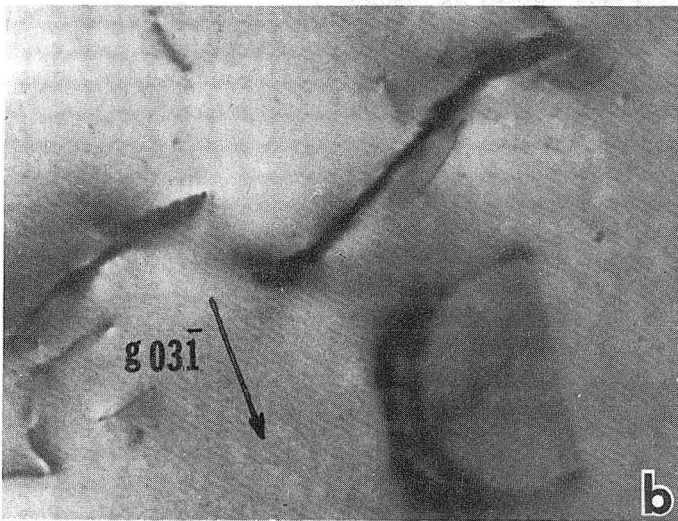
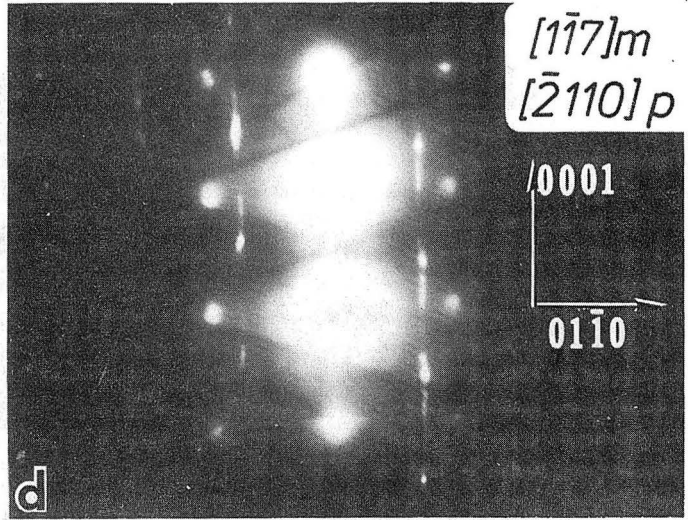
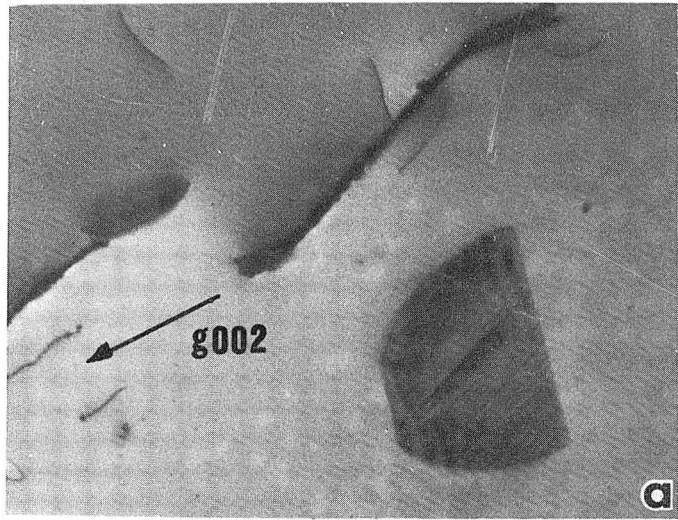
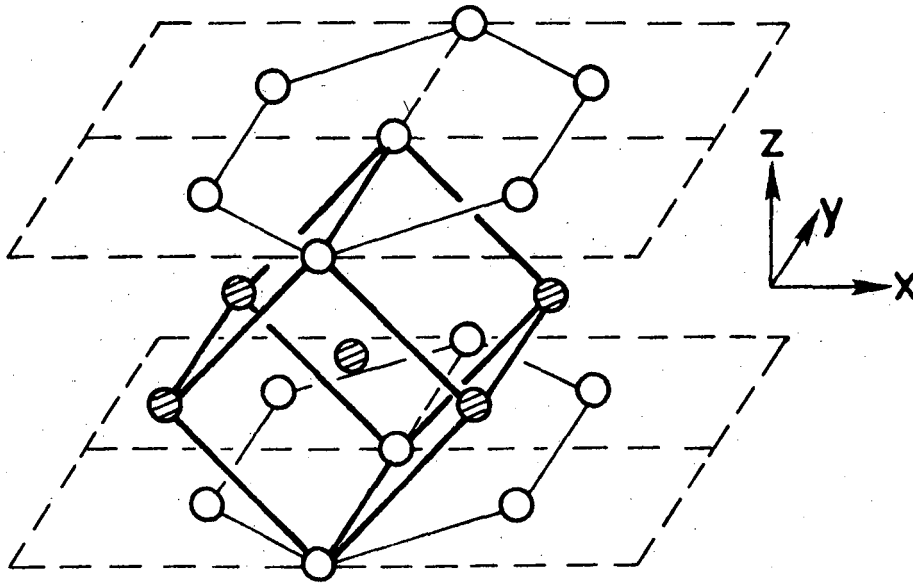


Fig. 5



XBL 828-11056

Fig. 6

This report was done with support from the Department of Energy. Any conclusions or opinions expressed in this report represent solely those of the author(s) and not necessarily those of The Regents of the University of California, the Lawrence Berkeley Laboratory or the Department of Energy.

Reference to a company or product name does not imply approval or recommendation of the product by the University of California or the U.S. Department of Energy to the exclusion of others that may be suitable.

TECHNICAL INFORMATION DEPARTMENT
LAWRENCE BERKELEY LABORATORY
UNIVERSITY OF CALIFORNIA
BERKELEY, CALIFORNIA 94720